Comparative Study of the Moon and Mercury: Rupes, their Topography and Origin

*Manabu Kato[1], Hisashi Ootake[1]

1. Institute of Space and Astronautical Science, Japan Aerospace Exploration Agency

Rupes of the Moon and Mercury are comparatively studied on their topography and origin. Images of rupes taken by Kaguya TC and MI, Lunar Reconnaissance Orbiter LROC for the Moon , and MESSENGER MDIS for Mercury are downloaded from Kaguya Data Archives and NASA Planetary Data System. The images are processed and mosaicked to investigate their feature and topography using USGS Integrated Software for Imagers and Spectrometers ISIS program package.
Thirty-one rupes on Mercury are described in IAU approved Gazetteer of Planetary Nomenclature. Only eight rupes of the Moon are named in the list. Rupes are characteristic and remarkable feature in Mercury surface thought to be originated when Mercury's interior cooled and the entire planet shrank slightly as a result. Most rupes in the Moon distribute in the outer edge of mares to attribute their origin to magma eruption. The rupes have never been found in lunar highland and farside except for Rupes Altai in nearside highland.
High resolution images and topographic data of rupes will be referred to show the difference of feature, topography, and origin in the Moon and Mercury.

Keywords: Kaguya, LRO, MESSENGER, rupes, ISIS, mosaics

Extension of the lunar Web-GIS “GEKKO”: Toward statistical analyses of the lunar spectral data

*Shota Iimura[1], Yoshiko Ogawa[1], Yohei Hayashi, Naru Hirata[1], Hirohide Demura[1], Tsuneo Matsunaga[3], Satoru Yamamoto[3], Yasuhiro Yokota, Makiko Ohtake[2]

1. University of Aizu, 2. Japan Aerospace eXploration Agency, 3. National Institute for Environmental Study

The Spectral Profiler (SP) is one of the 14 kinds of observation equipments onboard the Japanese lunar orbiter Kaguya. The spectra of lunar minerals generally have characteristic absorption bands in the observed wavelengths by the SP. By comparing the observed SP spectra with the absorption bands of the known minerals measured in laboratories, we can identify the minerals distributed at the observation spots on the Moon.
A lunar Web-GIS named GEKKO [Hayashi et al, 2016] (Moonlight in Japanese) is a visualization system for the SP data. The GEKKO displays SP observation footprints on the overall images of the Moon on the GIS screen. The users can view the SP spectra observed at the exact spots and download the data very easily just by clicking in the GEKKO system.
Sugimoto et al. [2014] focused on developing a framework for implementing analysis functions to the GEKKO. A few limited functions were implemented for the simplest and preliminary analyses in their study which are not so practical though.
The goal of this study is to extend the framework of Sugimoto et al. [2014] for further implementation of practical analysis functions in the GEKKO. We aim to implement new analysis functions practically used for the VIS-NIR spectral analysis and statistical data analysis. We prepared the extended new framework and succeed in implementing the functions of principal component analysis (PCA) and clustering analysis. Both analysis methods are very major in multivariable data analysis. They are useful for the spectral analyses to understand the distribution of the lunar minerals based on the globally observed data.
In the new framework, the analysis programs are modularized. So the provider can quickly and easily implement various kinds of analysis functions according to the users’ requests. Once such analysis functions are installed, selection or combination out of various kinds of analysis functions are very flexible and completely up to the users. The users see the analysis results quickly on the web site and can get back to check the original SP spectra very easily, too.
The analysis of SP data is essential for the mineral mapping of the Moon. The new framework and implementation of various kinds of analysis functions to the GEKKO is an important step for statistical analyses of the lunar spectral data toward global mapping of the mineral distribution.
.
References:
Hayashi, Y., Ogawa, Y., Hirata, N., Terazono, J., Demura, H., Matsunaga, T., Ohtake, M., Otake, H., "GEKKO" for Hyperspectral Data Distribution: A New Method for Utilizing the Advantages of a Web Map Service, 47th Lunar and Planetary Science Conference, LPI Contribution No. 1903, p.1920, 2016.
Sugimoto, K., Hayashi, Y., Ogawa, Y., Hirata, N., Terazono, J., Demura, H., Matsunaga, T. Yamamoto, S., Yokota, Y., Ohtake, M. Ootake, H., Development of a web application for dynamic analysis of the Kaguya Spectral Profiler data, Japan Geoscience Union Meeting 2014, Pacifico Yokohama, Japan, May 2014.

Keywords: GEKKO, Spectral Profiler, Kaguya, Geographic Information system , Principal Component Analysis, Cluster Analysis

Implementation of assortment algorithm for excluding noisy data in the lunar web-GIS: GEKKO

*Yuya Matsubara[1], Yoshiko Ogawa[1], Makiko Ohtake[2], Yohei Hayashi, Naru Hirata[1], Hirohide Demura[1], Tsuneo Matsunaga[3], Satoru Yamamoto[3]

1. University of Aizu, 2. Japan Aerospace eXploration Agency, 3. National Institute for Environmental Study

The lunar web-GIS “GEKKO” [Hayashi et al., 2016] is a very convenient system for the users to view the observed spectra on the Moon with the surface images. The main objective of developing the GEKKO is to display the Spectral Profiler (SP) data and visualize the information of the minerals brought out from the data. The SP is a spectrometer, onboard Kaguya which is a Japanese lunar orbiter. The SP observed the visible-near infrared reflected spectra of the lunar surface right under the satellite. We can identify the minerals and constrain the minerals the distribution on the Moon by detecting the absorption bands of the observed spectra. The web-GIS “GEKKO” plots observation footprints of SP on the lunar surface image. When users select any observation point, the GEKKO displays the graph of the SP spectra observed at the spot, the table to show ancillary data, and the high resolution image taken by imager, onboard Kaguya. The users can also download SP data very easily through this GEKKO system too. SP data analysis functions are also implemented in the GEKKO system recently. The analysis system has been installed by Sugimoto et al. [2014] and Iimura et al. [2017]. Sugimoto et al. [2014] developed a framework for real-time analysis of SP and implemented very simple functions of similarity analysis. Iimura et al. [2017] extended the framework of Sugimoto et al. [2014] and implemented practical functions:- principal component analysis (PCA) and clustering analysis. The current GEKKO is useful for viewing and analyzing SP data, however, the system uses and displays all the SP data amounting to about 70 million spectra which include noisy data. The S/N ratios of SP data depend on observation conditions. The noisy data should not be used for the analysis without caution. Especially, in statistical analysis such as PCA using a bunch of data, stacking of noise could affect the results critically and prevent with appropriate evaluation and understandings. Thus, this study tries to evaluate the noise first and develop the algorithm to classify the low-quality SP data. We developed and implemented the new function to discriminate low-quality data in the GEKKO. When users use this function, the data judged as of low-quality are shown by changing the colors of SP footprints where such noisy data are observed. The judgement criteria can be chosen by users flexibly. The users can also tune and adjust the controlling parameters for discriminating noisy data. Thereby, users can check quality of each SP data and select SP data with the higher S/N ratios according to user's objectives or preferences.

Keywords: moon, Kaguya(SELENE), Spectral Profiler, web-GIS, GEKKO, noise evaluation

Improvement of the extraction method of lunar secondary crater using the Voronoi tessellation

*Yuhi Yasuda[1], Chikatoshi Honda[1]

1. The University of Aizu

One of the estimation methods of formation age of planet surface is the crater chronology. Generally, craters are increasingly formed on the planet surface at random over time. From this perspective, the crater chronology utilizes the crater number density to estimate the formation age of planet surface. When we utilize the crater chronology, we should exclude secondary craters. Secondary craters are formed by ejecta thrown out from primary crater produced by the impact object from interplanetary space. The characteristic of secondary craters shape is clustered or chained with herringbone patterns. Thus, if we could not discriminate between primary and secondary craters, it causes an error of the estimation formation age. Although Kinoshita (2014) extracted lunar secondary craters based on the Voronoi tessellation of craters, some secondary craters were not extracted. Therefore, I tried to further develop the algorithm based on Kinoshita (2014) to extract such secondary craters and decrease the error between the result of my improvement method and the result of visual inspection. As a result of my improvement, the error between the result of my improvement method and the result of visual inspection is decreased by 15% compared with the method based on Kinoshita (2014).

Keywords: moon, secondary crater, the Voronoi tessellation

Positive openness map for visual inspection of fault scarp associated with lunar wrinkle ridges

*Tomokazu Sato[1], Chikatoshi Honda[1]

1. University of Aizu

Wrinkle ridges are topographic features observed often in plains of the moon. Both edges of wrinkle ridge have scarps related to the fault slip in the subsurface. According to a hypothesis of the origin of wrinkle ridges (e.g., Suppe et al., 1983), the scarps are defined as fore-limb and back-limb, and the fore-limb which has abrupt slope compared with back-limb corresponds to a fault scarp. These fault scarps are formed by horizontal pressure related to tectonic deformation of subsurface of the moon. The spatial distribution and their scale of fault scarps with wrinkle ridges lead us to understand the evolution of the lunar subsurface.
We applied the positive openness as a representative parameter of solid of the sky extent over a point of interest as a parameter for preparing effective data to identify candidates of fault scarps associated with wrinkle ridges. Positive openness map could be calculated from lunar Digital Terrain Model (DTM) acquired by Terrain Camera/Kaguya. Radial limit which is the range of positive openness calculation for the interest, affects the difference in vision of enhancement of topographic features. As a result of several radial limits calculations, we adopted radial limit of 222 m as a most appropriate one. By using of positive openness map, we could found several candidates of fault scarps associated with wrinkle ridges.

Keywords: moon, wrinkle ridge, positive openness map

Automatic detection of lunar sub-km craters via deep learning

*Riho Ito[1], Ryosuke Nakamura[1], Chikatoshi Honda[2]

1. National Institute of Advanced Industrial Science and Technology, 2. The University of Aizu

Crater chronology is a method that estimates generated age on surface of a body from size-frequency distribution (SFD) of impact craters. Coordinates and diameter are needed for computing SFD, and measurement accuracy of crater information is factored into the estimation accuracy of crater chronology. So, highly accurate crater information is important for discussing evolution process of the lunar surface. We can sufficiently detect smaller than 1km craters because spatial resolution of lunar observation data is improved, for example, resolution of Terrain Camera (TC) ortho data is 7.4m/pixel to 10.0m/pixel. TC ortho data were generated by SELENE observation data. However, manually detecting sub-km crater take an immense amount of time because number of crater is increase exponentially with decreasing crater diameter. For solving these tasks, automatically crater detection algorithms (CDAs) have been studied. Goal of these studies is to generate high accuracy crater information enough to apply crater chronology. For detecting martian craters from high resolution (12.5m/pixel) panchromatic imagery that was captured by High Resolution Science Camera aboard Mars Express spacecraft, Joseph et al. (2016) proposed a CDA with Convolutional Neural Network (CNN). CNN is part of deep learning methods. By designing the neural network architecture that has more multi layers, deep learning can represent the data more abstract. From supervised data, deep learning can learn optimal features that are needed for feature extraction process and data identification process. Especially, CNN keeps high performance in the field of computer vision (for example, image recognition, sound recognition). Joseph et al., (2016) reported that results of crater detection by using CNN get more high performance than other CDAs (Bandeira et al., 2010; Urbach and Stepinski, 2008).
Purpose of this research is to entertain sub-km CDA by using CNN with TC ortho imagery. By using high resolution imagery, to be able to detect smaller craters than before will be expected. A part of important things for deep learning is to prepare many supervised data. In this research, by detecting craters in manually, we prepared a crater dataset that includes 185 m to 1 km in diameter craters on Mare Imbrium(footprint of a TC ortho image: TCO_MAPm04_N24E333N21E336SC). The TC ortho image was divided into 3 regions (north, center and south). The crater datasets was detected by manually. The center region and the south region were used for learning, and the north region was used for evaluation. Input data for CNN were small patches that were cropped based on each crater diameter, and all patches were scaled 15 x 15 pixel. Positive sample is that craters are included, and negative sample is that craters are not included. In fact, CNN learned classifier task that “are there craters in a patch or not?” In this result, patch based classification accuracy was over 90 %. Additionally, we tried image based classification (crater detection from a part of north area image). In this result, CNN could detect position of craters, but could not detect shape and there were many false detections about object that has similar features to craters.

Keywords: Deep Learning, Crater Detection

Influence on illumination condition by analysis altitudes

*Inoue Hiroka[1], Hisashi Otake[1], Makiko Ohtake[1], Mitsuo Yamamoto[1], Takeshi Hoshino[1], Takanobu Shimada[1], Satoshi Tanaka[1], Koichi Masuda[1], Hitoshi Morimoto[1], Sachiko Wakabayashi[1], Tatsuaki Hashimoto[1]

1. Japan Aerospace Exploration Agency

The Japan Aerospace Exploration Agency (JAXA) launched a Moon orbiter, Kaguya, in September 2007 and succeeded in putting it into an orbit approximately 100 kilometers above the Moon in October. This Moon orbiter has provided us with a significant amount of scientifically valuable Lunar data. Besides Japan, various other countries all over the world have succeeded in obtaining Lunar observation data using Moon orbiters such as NASA’ s Lunar Reconnaissance Orbiter (LRO). The future objective of Moon exploration is to investigate the existence of volatiles such as water and sodium, and to search their potential usefulness. Since valuable resources are likely to exist in the lunar polar region, some countries are currently planning landing missions around the lunar poles. JAXA is also considering a Moon polar exploration mission whose purposes are to investigate the existence of lunar resources and to study their potential. For such a mission, we must select a landing site with long-term desirable sunlight conditions because the mission period is expected to be long due to the observation at the site. Illumination condition analysis of the south pole has been well studied, but that of the north pole is insufficient even though a superiority of the south pole for a landing site has not fully examined. Landing site selection is critical for the mission accomplishment in the polar region, so much previous work has well analyzed illumination conditions in the Moon polar region. The Moon has more undulating terrain than the Earth, so sunshine conditions change remarkably with the altitude or sunshade. Hence, we determine an appropriate landing site and calculate the illumination conditions for the landing site assuming three different altitudes.

We employed Digital Elevation Model (DEM) data obtained by the Lunar Orbiter Laser Altimeter (LOLA) of LRO and the Terrain Camera (TC) of Kaguya. In addition, we used the SPICE toolkit to calculate the position of the Sun. By combining the DEM data and Sun position, we can calculate the ratio of solar disc occulted by the horizon. We first conducted the simulation of illumination condition over a 60 km square around the lunar north pole. Within the good illumination condition area, there are especially favorable sites that satisfy the conditions for landing that the surrounding area also has good sunshine and smaller differences in height. For the candidate landing sites, we did not regard the Sun as one light source but separated it into 52 sun discs, and simulated illumination for altitudes of 0, 2, and 5 meters.Figure represents changes of sun visibility with each altitude. The colorbar shows the number of sunshine days in two years.

We present the illumination simulation results of an especially favorable landing site using LRO and Kaguya data. We can obtain the detailed sunshine conditions or its difference with altitude by conducting simulation with changing altitude. Future work will focus on the illumination simulation for a wider range of regions for precise landing site selection. In addition, we must evaluate the influence of resolution of input DEM data on illumination conditions.

Keywords: Moon, Analysis of illumination conditions, Polar region

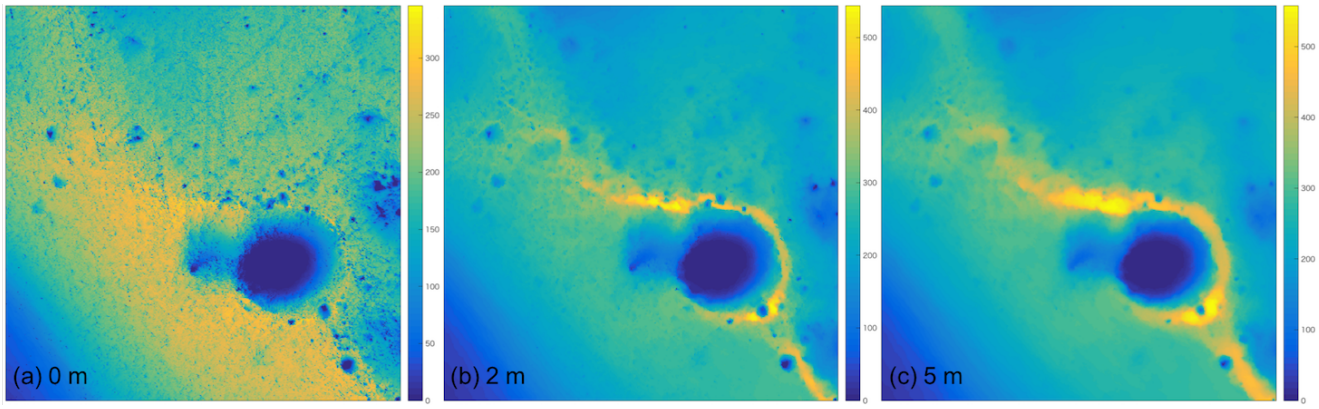

Geological map of Mare Smythii based on the SELENE observation data

*Ken Ishiyama[1]

1. Institute of Space and Astronautical Science, Japan Aerospace Exploration Agency

Lunar geological map is useful for understanding the process of lunar tectonics and volcanic activity, so the high-resolution terrain and spectral cameras has updated the lunar geological map day by day [e.g., Brennan, 1975; Hiesinger et al., 2010]. Thus, these surface information produced the present lunar geological map, but on which, the subsurface information was not reflected. This information gives the subsurface structure, its stratigraphy, and the thickness of subsurface lava flow layer, so becomes important clue of lunar tectonics and volcanic activity.
In this study, I focused on Mare Smythii, which is located at 2˚S, 87˚E on the Moon. The surface of Mare Smythii is covered only by one lava flow, which erupted ~3.14 Ga ago [Hiesinger et al., 2010]. According to the SELENE/Lunar Radar Sounder observation, the several subsurface boundaries were founded in Mare Smythii [Ono et al., 2009; Kobayashi et al., 2014]. The part of subsurface boundary outcropped on Mare Smythii, so we concluded that the surface of Mare Smythii was composed of two lava flows at least; the subsurface information succeeded in updating the geological map of Mare Smythii. In the presentation, I will report the preliminary geological map of Mare Smythii.

Distribution of Olivine and Plagioclase around the Crisium Basin on the Moon

*Yuji Agatsuma[1], Naru Hirata[1]

1. The University of Aizu

Global distribution of purest anorthosite (PAN) and olivine on the Moon has been revealed (Ohtake et al., 2009, Yamamoto et al., 2010, 2012), but mineral distribution on certain local regions have not often been discussed. Detailed analysis on local regions is also important to examine the lunar crustal structure. Sugamiya and Hirata (2015) revealed distribution of olivine, plagioclase and pyroxene in the southwest rim of the Crisium basin where the existence of these minerals were previously reported (Yamamoto et al., 2010, 2012). They used Multiband Imager (MI) data onboard SELENE (Kaguya). MI has high spatial resolution and it enables us to examine the whole region of the moon without gap. In this study, we expand the target region of their work to whole sector by investigating distribution of olivine and plagioclase around the Crisium basin using same method as Sugamiya and Hirata (2015). We found a wide and homogeneous distribution of olivine and plagioclase around the Crisium basin. As Sugamiya and Hirata (2015) have already been stated, sites of these minerals are associated to small craters around the basin. We found that the CSFD for craters associating olivine site almost matches the isochron for 3.44 Ga, expected age of the Crisium basin, in the size range of over 6 km in diamter. This means that olivine can be detected in almost all craters larger than 6 km in diameter, and olivine is commonly distributed in the ejecta of the Crisium basin beneath over 600 m from the surface.

Keywords: Lunar crust, olivine, plagioclase, Multiband Imager

Study on lunar Mg, Fe and carbon-bearing rocks formed at extreme condition

*Yasunori Miura[1]

1. Visiting (Yamaguchi, AIC University)

The Moon has been discussed as to whether it has evolved from water-Earth or is an unique Earth planet compared to air-planets of Mars and Venus, or water-planet Earth. Author studied in present study is based on recent model that the Moon produces local gas and fluids remained on surface basaltic rocks with carbon-volatiles but without global active system, which is main purpose of the present paper as follows.

1. Solid rocks in any celestial bodies (including the Moon basically) have been accumulated from nano-particle to macro-grains by evaporating volatile-elements as buffer roles above the solidified rocks.
2. There are three types of global systems in the Earth-type planets. The solid rock system is remained globally by various collision phenomena, but generation of local gas or liquid states above the rock. Mars and Venus have global air-system, and our Earth has global air- and water-systems above the solid rock as different planets.
3. Carbon-bearing solidified grains exist in fine scale widely during the three-state changes of celestial bodies development. The carbon can be remained during extreme condition by exchanged states state, which suggests that the elemental abundance of carbon element is richer in quenched carbonaceous chondritic meteorite than the crust rocks of Earth clearly. The carbon-bearing solid grains is considered to be an "extreme-condition (shocked) indicator" showing active state change.
4. Lunar basaltic rocks show high Mg, Fe and carbon contents in the Apollo lunar and meteorite samples. The basalts are therefore volcanic rocks solidified on the surface in the extreme state of meteoritic impacts on the primordial periods of the Moon. Basaltic compositions formed by extreme condition are difficult to be distinguished from the surface shallow or deep interior of mantle origins at the present evolved today. The carbon element mixed in the solidified grains during basaltic formation can be found as high pressure-type carbons (as diamond sources) now, where volatile carbon can be found even in deep interior today. Quenched rock containing carbon-bearing fine grains can be observed by nanotechnology with an high-sensitive electron microscopy, which will be shown in author’ s presentation in the plenary session of the JpGu-AGU 2017.

The present study can be summarized as follows. 1. The basaltic rocks on the lunar surface can be pointed out from the bulk compositional characteristics formed in the extreme impact condition. 2. Fe, Mg and carbon are remained in the rock surface of the shocked glassy solids. 3. Carbon-bearing fine grains called here as "extreme-condition (shocked impact) indicator" can be observed on the solidified surface rocks. 3. Igneous rocks formed by the impact process are widely formed on the shallow surface of a celestial body to deep interior during its evolution process finally, which can be also applied to the igneous rocks contained carbon volatiles in the mantle rocks globally. 4. The present results of primordial basaltic rocks with carbon remnants indicate that there is no global fluid ocean water-Earth system in the Moon and other planets relatively.

Keywords: Carbon-bearing grains, The Moon, Basalt

U-Pb systematics of lunar meteorite NWA 2977

*Narumi Moromoto[1], Kentaro Terada[1], Yosuke Kawai[1], Masaaki Miyahara[2], Yuji Sano[3], Naoto Takahata[3]

1. Osaka University Graduate School of Science, 2. Hiroshima University Graduate School of Science, 3. Atmosphere and Ocean Research Institute, The University of Tokyo

The lunar meteorites are important because they would give us a new insight into the unexplored region of the Moon. North West Africa (NWA) 2977 is identified as olivine cumulate lunar meteorite, which was discovered in Morocco in 2005. So far, we have found a remarkable shock melt vein (SMV) in the thin section, which had suffered from the impact melting and rapid cooling.
In this study, in order to investigate the thermal history of NWA 2977, we carried out the in-situ U-Pb dating of phosphate grains in/out of the SMV, using Nanoscale Secondary Ion Mass Spectrometer (NanoSIMS) at the Atmosphere and Ocean Research Institute, University of Tokyo. Most of the phosphates give a crystallization age of 3132±67 Ma (1 σ). Whereas, one grain out of the SMV shows a slightly disturbed U-Pb systematics, indicating the very recent shock event (< 346 Ma). At the conference, we also discuss μ-value ($^{238}U/^{204}Pb$) of NWA2977.

Role of volatiles during late-stage crystallization of intercumulus pockets: Comparison of the NWA 773 clan of lunar meteorites with terrestrial gabbro from Murotomisaki, Japan

*Timothy Fagan[1], Jun Uchida[1], Takatsugu Asahi[1]

1. Department of Earth Sciences, School of Education, Waseda University

Introduction: Late-stage intercumulus pockets in the olivine cumulate (OC) lithology of the Northwest Africa 773 clan of lunar meteorites are enriched in incompatible elements [1]. Pyroxene crystals adjacent to the pockets are zoned, with Ti# (Ti/[Ti+Cr]) increasing and Fe# (Fe/[Fe+Mg]) remaining constant as the pockets are approached, providing an example of igneous differentiation on the Moon [1]. The pockets are also of interest because they typically contain the Ca-phosphates merrillite and apatite; apatite crystals in the pockets contain F, Cl and OH in various ratios, reflecting the composition and abundance of volatile elements during late-stage crystallization of the OC [2-4]. The presence of H_2O in the apatite indicates that water was present in pockets of residual liquid trapped in the OC; however, the abundance of water and effect of water on late-stage crystallization have not been resolved.
In this study, we (1) compare late-stage pockets of NWA 773 clan OC with pockets in terrestrial gabbro from a sill in Murotomisaki, Japan [5], and (2) determine F:Cl:OH ratios in lunar apatite using low-voltage EPMA (electron probe micro-analysis; see below). The main goals are to evaluate and compare the roles of volatiles, particularly water, during late-stage crystallization in lunar and terrestrial gabbros.
Methods: We compared minerals and textures of late-stage pockets from the Murotomisaki sill with pockets from NWA 2977 and NWA 773. In this study, our main observations are based on one sample (Muro-14) collected from the coarse gabbro unit in the central part of the sill [5]. We compared Muro-14 with a polished thin section (pts) of NWA 2977, which is part of the NWA 773 clan and consists entirely of OC [6,7]. Images of minerals and textures were collected using petrographic microscopes, SEM (BSE images, Hitachi S-3400N) and EPMA (BSE and x-ray elemental maps, JEOL JXA-8900). Major element compositions in feldspar were collected by EDS using the SEM and by WDS using the EPMA. Changes in feldspar composition were compared to distance from pockets.
Determining the ratios of F, Cl and OH in apatite is difficult because F and Cl K-alpha X-rays typically vary during exposure to an electron beam [8] and OH cannot be detected by EPMA. So, we have been developing an EPMA technique (in collaboration with D. Harlov; see [9]) that uses low voltage (7 kV) to limit variations in F and Cl count rates. A small spot size (~ 1 μm) is desired because of the small grain size of much apatite in NWA 773.
Results: In both Muro-14 and NWA 2977, plagioclase is zoned, with more Ab-rich compositions closer to the pockets. In NWA 2977, feldspar varies from Ab_{05} to Ab_{15}, whereas the Muro-14 feldspar is much more albitic (Ab_{40} to Ab_{95}). Discontinuities in zoning and porosity in feldspar closest to the Muro-14 pockets suggest that H_2O-rich fluid from the pockets interacted with feldspar, resulting in albitization. Some discontinuities also occur in NWA 2977, but it is not known if feldspars adjacent to pockets in NWA 2977 interacted with a volatile-rich fluid.
Most analyses of apatite in NWA 773 are F-rich, but variations in F/Cl at low OH and F/OH at low Cl occur in different petrologic settings. Data from [2] combined with our results show that NWA 773 OC pockets vary in F/OH at low Cl, suggesting some enrichment in H_2O during late-stage formation of the pockets.
References: [1] Fagan T.J. et al (2014) GCA 133: 97-127. [2] Tartese R. et al (2014) MaPS 49: 2266-2289. [3] Boyce J.W. (2014) Science 344: 400-402. [4] Asahi T. (2016) Goldschmidt Conference Abstracts 115. [5] Hoshide T. et al (2006) J. Min. Pet. Sci. 101: 223-239. [6] Zhang A-C. et al (2011) MaPS 45:

1929-1947. [7] Nagaoka H. et al. (2015) Earth Planets Space 67: 200, 1-8. [8] Stormer J.C. et al (1993) Am. Min. 78: 641-648. [9] Schettler G. et al (2011) Am. Min. 96: 138-152.

Keywords: gabbro, volatile elements, water

Performance of the pyroelectric X-ray generator developed for active X-ray spectrometer on future lunar and planetary landing missions

*Hiroshi Nagaoka[1], Nobuyuki Hasebe[1,2], Masayuki Naito[2], Miho Mizone[2], Haruyoshi Kuno[1]

1. Research Institute for Science and Engineering, Waseda University, 2. School of Advanced Science and Engineering, Waseda University

Planetary landing missions to the Moon and Mars have been recently performed. In Japan, future lunar landing mission have been also planned. The landing missions investigate the geology at landing site in detail. One of powerful methods to determine the elemental composition of the planetary surface is X-ray fluorescence spectrometry. We have developed active X-ray spectrometer (AXS) in order to apply the AXS for future lunar landing mission as elemental analyzer. The AXS consists of pyroelectric X-ray generators (PXG), and a silicon drift detector (SDD). Laboratory experiments have been conducted to obtain enough X-ray intensity from PXG to measure the major and important elements as Mg, Al, Si, K, Ca, Ti and Fe in short observation interval. Furthermore, we have developed a prototype of PXG with a high intensity of X-ray. In this work, the development and performance of present PXG will be reported and discussed.

Keywords: XRF, element

INTERNAL STRUCTURE OF THE MOON INFERRED FROM APOLLO SEISMIC DATA, SELENODETIC GRAIL AND LLR DATA AND THERMODYNAMIC CONSTRAINTS

Ekaterina Kronrod[1], *Koji Matsumoto[2], Ryuhei Yamada[3], Oleg Kuskov[1], Victor Kronrod[1]

1. Vernadsky Institute of Geochemistry and Analytical Chemistry (GOKHI RAS), 2. RISE Project, National Astronomical Observatory of Japan, 3. The University of Aizu, Research Center for Advanced Information Science and Technology

In the recent paper (1) lunar interior models by complementing Apollo seismic travel time data with selenodetic data which have recently been improved by GRAIL and LLR. Important information on the thickness of the crust, LVZ, core structure and seismic velocities was obtained. But this problem statement retains lunar mantle composition to be uncertain. In (2,3) mantle composition can be simulated based on thermodynamic approach and petrological evidence from seismic data, MOI and mass. The goal of this paper is to investigate lunar internal structure models which are consistent with the seismic and the selenodetic (GRAIL and LLR) data and thermodynamic constraints.

We apply spherically symmetric viscoelastic hydrostatic model of the Moon (1). The Moon consists of nine layers: megaregolith, crust, four-layers mantle, low viscosity zone (LVZ), liquid outer core and fluid inner core. In each zone physical properties are assumed to be constant. We employed same data as (1): four selenodetically observed data of mean radius, mass, MOI, and tidal Love number *k2* (4). Seismic travel time data was selected by (5).

Geochemical models of bulk Al and Fe composition: Currently there are two main groups of geochemical models of the Moon (6): 1. Moon's composition with Al content similar to models with Earth's Al_2O_3 content; 2. The Moon is enriched in Al against Earth. We consider models with Earth's Al_2O_3 content. Analysis of majority of current Moon's composition models (6) revealed that for group 1 Al_2O_3 = 4,05 ± 0,36 wt.% and Fe_2O_3 = 12,25 ±1,33 wt.%. Division mantle into 4 layers was performed according to (7) model. Concentrations of main oxides were equal in first 3 upper mantle layers (Mantle 1-3 in Fig.1) and we applied the model of magma ocean to calculate oxide concentrations in fourth lower mantle layer (Mantle 4 in Fig.1) (which implies that concentrations of main oxides in the lower mantle is equal to average concentrations in upper mantle and crust and equal to bulk concentrations). The models of the magma ocean in such a formulation were considered in our previous work (3). Temperature in the lunar mantle is defined by equation from (8).

Thermodynamic approach: The general our methodology is to combine the geophysical and geochemical constraints and thermodynamic approach, and to develop, on this joint basis, the self-consistent models of the Moon. The crustal composition of Taylor (1982) are taken as representative of the crust material. Thermodynamic modeling of phase relations and physical properties in the multicomponent mineral system CFMAS was used to develop a method for solving the inverse problem [3].

Inversion: A Bayesian inversion approach is an effective method to solve for a nonlinear problem such as planetary internal structure modeling, e.g., [7], [9]. The solutions of the parameters and their uncertainties are obtained from the posterior distribution which is sampled by the MCMC algorithm. In the present model bulk Al content and bulk Fe content are included into likelihood function (LHF).

Results: The main results are shown in Fig.1. Probable concentration of Al_2O_3 is 2,7-2,9 wt.% in the upper mantle and 4,1-4,3 wt.% in the lower mantle. Bulk Fe_2O_3 is within 11,5-12,5 wt.%. Seismic P-wave velocity (~7,92 km/s) in the lower mantle is close to lower bound of velocity range from (7). From these results it can be concluded that the models of the Moon with Earth's bulk Al content is in a good agreement with geophysical data.

References: [1] Matsumoto et al. (2015),GRL, 42, i18, 7351–7358; [2] Khan et al.(2007), Geophys. J.,168, 243–258; [3] Kronrod, Kuskov (2011) Izvestiya. Phys. Solid Earth (Rus), 47, 711-730; [4] Williams J. G. et al. (2014) *JGR, 119*, 1546- 1578; [5] Lognonne P. et al. (2003) *EPSL, 211*, 27-44; [6] Kuskov O.L.et al. (2014) *PEPI*, 236, 84-95; [7] Gagnepain-Beyneix et al. (2006) PEPI,159,140–166; *[8] E. V. Kronod et al.* (2013), Solar System Study: 4M-S3 IKI RAN,94-104.

Keywords: Moon, internal structure, numerical simulation, thermodynamics, composition

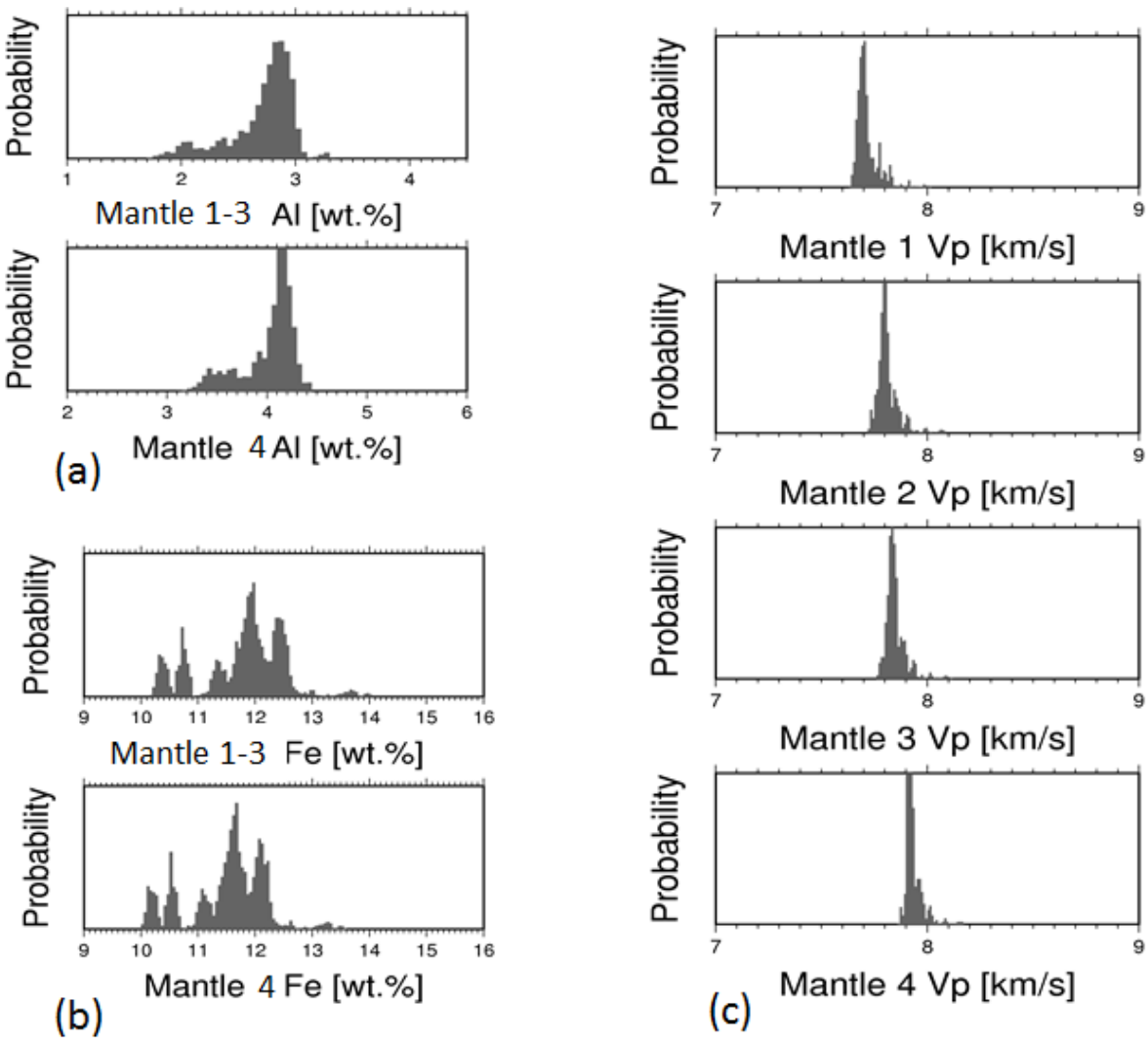

Fig. 1 Posterior probability density functions: Al (a) and Fe (b) concentrations and P-wave seismic velocities distribution in layers 1-4 of the lunar mantle.

NUMERICAL SIMULATION OF LUNAR SURFACE CHARGING AND ELECTROSTATIC DUST LOFTING DUE TO SOLAR WIND AND UV IRRADIATION

*Necmi Cihan Orger[1,2], J. Rodrigo Cordova Alarcon[1,2], Kazuhiro Toyoda[1,2], Mengu Cho[1,2]

1. Kyushu Institute of Technology, 2. Laboratory of Spacecraft Environment Interaction Engineering

The interaction with the surrounding plasma has several effects on the Moon, and one of them is suggested as electrostatic transportation of the lunar dust grains while the lunar surface is simultaneously charged by the continuous flux of the ambient plasma and the solar irradiation. The lunar surface emits photoelectrons when it is exposed to the solar ultraviolet and X-ray radiation, and this photoemission current establishes a current balance with the secondary electron emission and the collection of electrons and ions from incoming plasma. Since the Moon orbits the Earth under the solar wind influence most of the time, the upstream plasma conditions are typically driven by the solar activity. In addition, the lunar surface potential, electric field and Debye length change with variations in solar wind conditions, and the lunar dust grains can be lofted and/or levitated above the surface according to the current sources. Therefore, the conditions of fast and slow stream solar wind as well as post-shock plasma, early CME and late CME passages are investigated in order to figure out how the lunar dust particles can reach higher altitudes in this study. In addition, the electrostatic forces acting on the submicron-sized lunar dust particles are compared to the gravity and cohesive forces. Through the numerical simulations of the lunar surface and dust charging, the following outcomes were obtained. First, it has been observed that solar flare events produce strong electric field on the dayside of the Moon, and the dust grains can travel through dense and thin plasma sheath above the dayside surface. Second, very cold and low-density plasma, which can be seen during early CME passages, creates large positive potentials on the subsolar point similar to the solar flare events. Third, the results showed that strong electrostatic forces are not sufficient solely to loft the dust particles to higher altitudes since the time to travel through the plasma sheath above the surface is important to accelerate the charged dust grains to proper velocities. Lastly, the post-shock plasma limits the positive charging of the subsolar point while it increases the electrostatic force acting on the dust grains above the terminator region.

Keywords: lunar dust, lunar surface charging, dust lofting, solar wind, coronal mass ejection

Science Objectives and Status of the Next Generation Lunar Retroreflector

*Douglas G Currie[1], Giovanni Delle Monache[2], Bradford Behr[1], Simone Dell'Agnello[2]

1. Department of Physics, University of Maryland, College Park, USA, 2. INFN-LNF, Frascati, Italy

The design performance of the Next Generation Retroreflector (NGR), also known as the Lunar Laser Ranging Array Retroreflector for the 21st Century and/or MoonLIGHT depends critically on a detailed thermal analysis to optimize the design. This consists of three phases. The first, which will be the primary focus of this talk, consists of optimizing the performance with respect to the physical parameters of the package, conductivity, emissivity and reflectivity of various elements. This will be the primary focus of this talk, illustrating some initially surprising results. The second consists of optimizing the parameters of the CCR (the back angle offsets) in the presence of phase 1 conclusions. The third phase consists or readdressing the physical parameters of the package at the optimized back angle offsets. Updates on other issues will be briefly addressed: future landing sites and the required of a new design for the NGR,

Current status of the Next Generation Retroreflector (NGR) will be described. This will address the current schedule and future landing sites. In addition, interesting effects that have been recently discovered concerning break-through in solid CCRs, thermal effects in the CCR that affect the return signals, detailed simulations of the effects of atmospheric propagation and a candidate for a low absorption high emissivity coating will be briefly considered.

Keywords: Lunar Laser Ranging, Next Generation Lunar Retroreflector, Thermal Simulation

